

Phonon-Magnon coupling in CoF_2 investigated by time-of-flight neutron spectroscopy

Tapan Chatterji¹, Mohamed Zbiri¹, Stephane Rols¹

¹*Institut Laue-Langevin, B.P. 156,
38042 Grenoble Cedex 9, France*

(Dated: November 12, 2018)

We report the results of inelastic neutron scattering investigation on the model antiferromagnet CoF_2 by time-of-flight neutron spectroscopy. We measured the details of the scattering function $S(\mathbf{Q}, \omega)$ as a function of temperature with two different incident neutron wavelengths. The temperature and Q dependence of the measured scattering function suggests the presence of magnon-phonon coupling in almost all branches. The present results are in agreement with the strong magnetoelastic effects observed previously.

PACS numbers: 75.25.+z

The lattice dynamics of a crystal is normally assumed to be independent of the spin dynamics of the magnetic moments associated with the atoms and ions of the crystal. Similarly while describing the motions of the spins in a magnetically ordered systems it is usual to assume that the equilibrium positions of the magnetic ions are frozen. The approximation gives a fairly well description of the magnetic system and is in the same spirit as the adiabatic or Born-Oppenheimer approximation which is normally used for band structure calculations. In this approximation the phonon and magnons are separate entities with their own dispersion relations and the Hamiltonian of the system separates out into a lattice and a magnetic part. In reality however there always exists a coupling term that involves displacements both in the positions of the atoms in the crystal and in the orientations of the spin vectors associated with these atoms. Thus the collective excitations are neither pure lattice waves nor spin waves but rather magnetoelastic waves. Such magnetoelastic waves are predicted to exist theoretically long time ago¹. With the advent of enormous progress in first-principle calculations it is now possible to do phonon calculations of magnetic solids in the magnetically ordered phase by taking spin degrees of freedom into account. The difference between the results of the calculations done by taking and not taking magnetic degrees of freedom into account can be often very significant as has been amply demonstrated by such recent calculations on Fe-arsenide compounds². It is possible to study magnetoelastic effects experimentally by using neutron scattering techniques. Our recent neutron diffraction investigations^{3,4} have shown strong static magnetoelastic coupling in transition metal difluorides MnF_2 , FeF_2 , CoF_2 and NiF_2 . There exist indirect evidences for dynamic magnetoelastic or phonon-magnon coupling in FeF_2 , CoF_2 and NiF_2 ^{5,6}. However, a systematic study of the phonon-magnon coupling in this relatively simple system is still missing.

CoF_2 belongs to the family of transition-metal difluoride, which has been the subject of intensive investigations¹⁸⁻²⁵. CoF_2 , along with other transition-metal oxides MnF_2 , FeF_2 and NiF_2 , crystallize with the

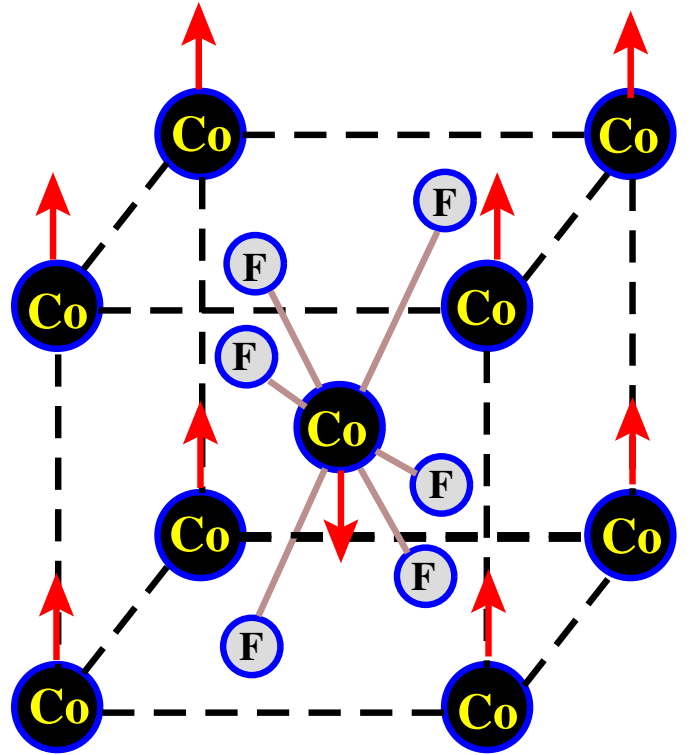


FIG. 1: The antiferromagnetic structure adopted by $3d$ transition metal difluorides viz. CoF_2 with the rutile type crystal structure. The Co and F ions are labeled. The arrows on the Co represent moment direction of the transition metal ions below the Néel temperature³¹.

tetragonal rutile-type structure in the $P4_2/mnm$ space group. However the magnetic properties of CoF_2 are more complex than those of isomorphous MnF_2 , because the Co ion has unpaired angular momentum that plays an important role in determining its magnetic properties. CoF_2 orders²⁶⁻³⁰ below $T_N \approx 39$ K with an antiferromagnetic structure³¹, shown in Fig. 1, with the propagation vector $\mathbf{k} = 0$. The magnetic moments of Co ions at the corner (000) positions of the tetragonal unit cell are all parallel to the c -axis whereas those of the Co

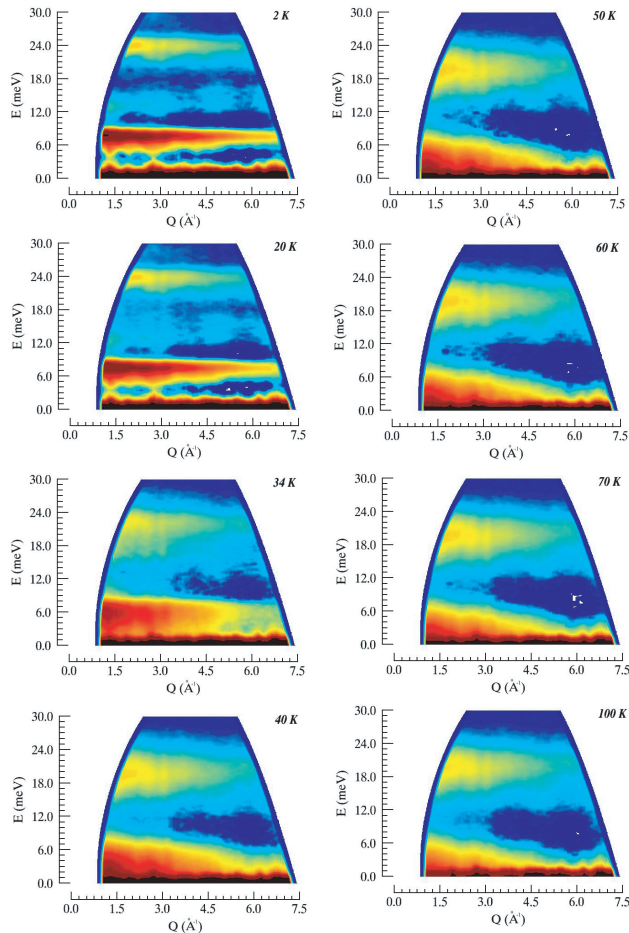


FIG. 2: (Color online) Temperature evolution of the scattering function $S(Q, \omega)$ measured from CoF₂ using incident neutron wavelength of $\lambda = 1.5 \text{ \AA}$.

ions at the $(\frac{1}{2} \frac{1}{2} \frac{1}{2})$ positions are oppositely oriented. The presence of an orbital moment in CoF₂ makes it particularly interesting for the study of magnetoelastic coupling in this compound. We recently investigated³² the hyperfine interaction in CoF₂ by high resolution neutron spectroscopy and concluded that the presence of the unquenched orbital moment of the Co ion in CoF₂ leads to its anomalous behavior compared to that of other Co-based compounds.

We have performed inelastic neutron scattering investigations on CoF₂ using the thermal time-of-flight neutron spectrometer IN4C at the Institute Laue-Langevin in Grenoble. About 5 g of CoF₂ powder sample was put inside a cylindrical Al sample holder that was fixed to the cold tip of the sample stick of a standard orange cryostat. In order to cover an extended Q -range, relevant to the present study, and to gain in energy resolution two incident wavelengths of $\lambda_i = 1.1$ and 1.5 \AA , respectively, were used. This allowed the Stokes spectrum to be measured at low temperature over a broader dynamical range. The data analysis was done using ILL software tools

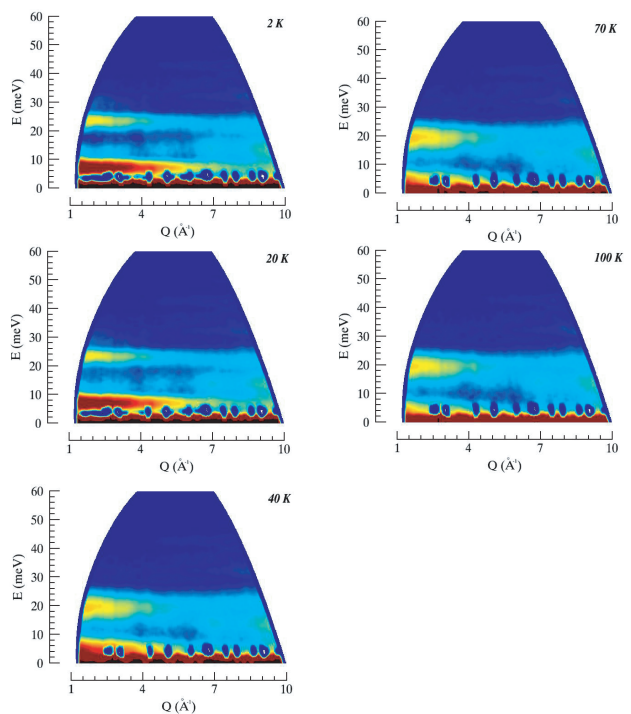


FIG. 3: (Color online) Temperature evolution of the scattering function $S(Q, \omega)$ from CoF₂ measured with the incident neutron wavelength of $\lambda = 1.1 \text{ \AA}$.

The present investigations have been performed with unpolarized neutrons on powder samples of CoF₂. The present method is therefore somewhat limited because it gives only the powder average results and does not give information of detailed directional Q dependence. Also the unpolarised neutron scattering cannot distinguish directly whether the scattering is of magnetic or structural origin. However and since CoF₂ contains magnetic Co ions, we can therefore expect inelastic magnetic scattering due to the interaction of the neutron spin with the spin and orbital magnetic magnetization of the CoF₂ both below and above the magnetic ordering temperature $T_N \approx 39 \text{ K}$. Also the neutron is sensitive to the structural excitations or phonons which exist at all temperatures. Thus this technique will measure both excitations and even highlights their hybrid feature described before. Magnetic and structural excitations have fortunately different temperature and Q dependence. Strong and sharp inelastic magnetic excitations are expected only below the magnetic ordering temperatures. At higher temperature, the magnetic correlations give broad quasielastic

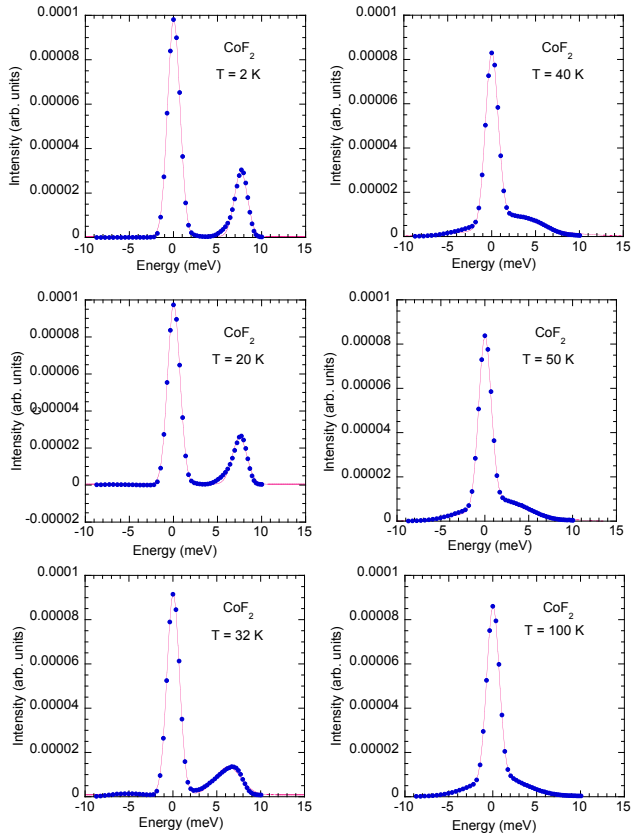


FIG. 4: Results of the fit of the low-Q data (integrated over Q in the range from 0.9 to 3.56 \AA^{-1}) from CoF₂ in the low-energy range ($\lambda_i = 1.5 \text{ \AA}$). Two Gaussian peaks have been fitted to the elastic peak at zero energy and the inelastic peak which is at about $E = 8 \text{ meV}$ at $T = 2 \text{ K}$. The energy of inelastic peak decreases with increasing temperature and becomes zero at $T_N = 38 \text{ K}$ giving rise to quasielastic scattering which has been fitted with a Lorentzian function.

scattering instead. The intensity of the magnetic excitation peaks decrease with the momentum transfer Q. The scattering due to structural excitations or phonons have different temperature and Q dependences. The phonon intensity in general increases with increase of the momentum transfer Q. Of course intensities of magnons and phonons are also governed by the magnon and phonon structure factors and also polarisations which depends on the details of the magnetic and crystalline structures. However the differences in temperature and Q dependence for magnons and phonons can be conveniently used for the sake of identification in order to separate them.

The cross section for neutron scattering by magnetic systems is discussed in details in several text books on neutron scattering^{33,34}. The expression for neutron scattering cross sections are very complex when the ions have both spin and orbital angular momentum. It can be

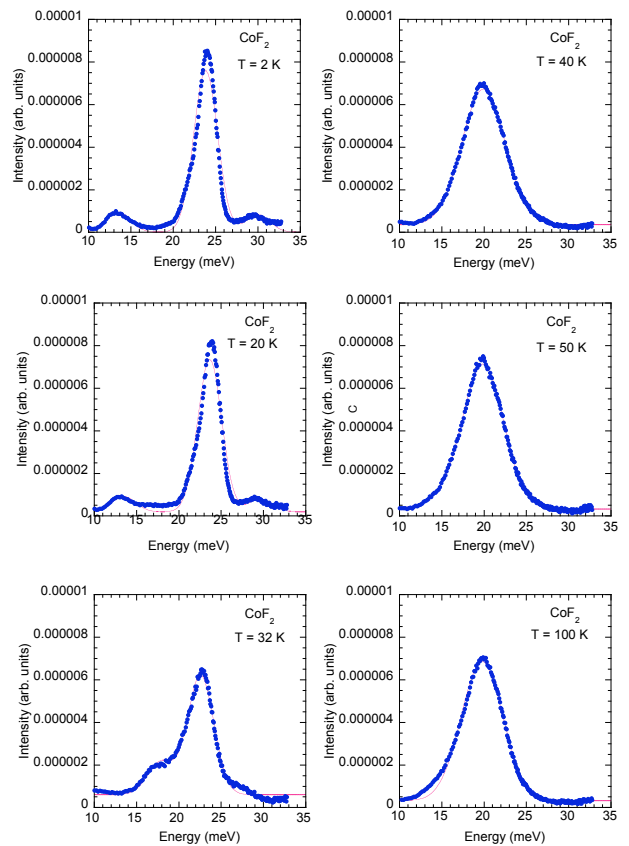


FIG. 5: Results of the fit of the low-Q data (integrated over Q in the range from 0.9 to 3.56 \AA^{-1}) from CoF₂ in the higher-energy range ($\lambda_i = 1.5 \text{ \AA}$). At low temperatures below $T_N = 38 \text{ K}$, three peaks could be identified and they were fitted with three Gaussian functions. At higher temperature only a broad peak could be identified and has been fitted with a single Gaussian function.

greatly simplified if the momentum transfer is less than the reciprocal of the radius of the magnetic shell and is given by

$$\frac{d^2\sigma}{d\Omega d\omega} = \frac{k_f}{k_i} \frac{1}{2\pi} \left(\frac{1.91e^2}{2mc^2} \right)^2 \quad (1)$$

$$\times \sum_{ij} |f(\mathbf{Q})|^2 \int_{-\infty}^{\infty} \langle \mathbf{K}(i, 0) \cdot \mathbf{K}(j, t) \rangle$$

$$\times \exp[i\mathbf{Q} \cdot (\mathbf{R}(i) - \mathbf{R}(j))] \exp(-i\omega t) dt,$$

where $f(\mathbf{Q})$ is the form factor of the ions, $\mathbf{K}(j, t)$ is the part of the magnetic moment operator, $\mathbf{L} + 2\mathbf{S}$, which is perpendicular to \mathbf{Q} , for the ion i at $\mathbf{R}(i)$ at the time t , \mathbf{k}_i and \mathbf{k}_f are the wavevectors of the incident and scattered neutrons.

The neutron scattering cross section of a phonon mode

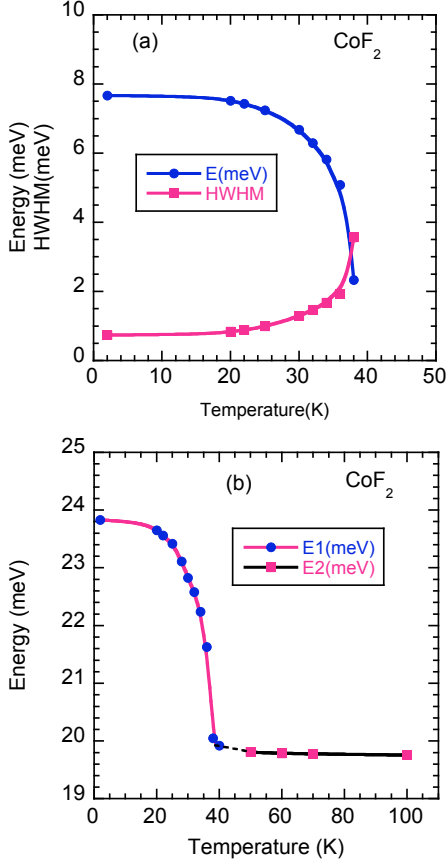


FIG. 6: (Color online) (a) Temperature variation of the energy and the half-width at half-maximum (HWHM) of the low-energy inelastic magnetic peak of CoF₂. (b) Temperature variation of the energy of the high-energy inelastic magnetic peak of CoF₂ ($\lambda_i = 1.5 \text{ \AA}$).

($\mathbf{q}j$) is given by

$$\frac{d^2\sigma}{d\Omega d\omega} = \frac{k_f}{k_i} \frac{1}{\omega(\mathbf{q}j)} \quad (2)$$

$$\left| \sum_k \left(\frac{\hbar}{2M_k} \right)^{\frac{1}{2}} b_k \mathbf{Q} \cdot \mathbf{e}(k, \mathbf{q}j) \right.$$

$$\times \exp[i(\mathbf{Q} - \mathbf{q}) \cdot \mathbf{R}(k)] \exp(-W_k(\mathbf{Q})) \left. \right|^2$$

$$\times \left(\frac{n(\mathbf{q}j)}{n(\mathbf{q}j) + 1} \right)$$

where $\exp(-W_k(\mathbf{Q}))$ is the Debye-Waller factor for the k th atom, $n(\mathbf{q}j)$ is the population of the mode and is taken for neutron energy loss, b_k is the scattering length of the k th atom in the unit cell, M_k its mass, and $\mathbf{e}(k, \mathbf{q}j)$ is the eigen vector in the normal mode ($\mathbf{q}j$). Note that everything we stated in the previous section about the different Q dependence of the magnons and phonons, follows directly from equations (1) and (2)

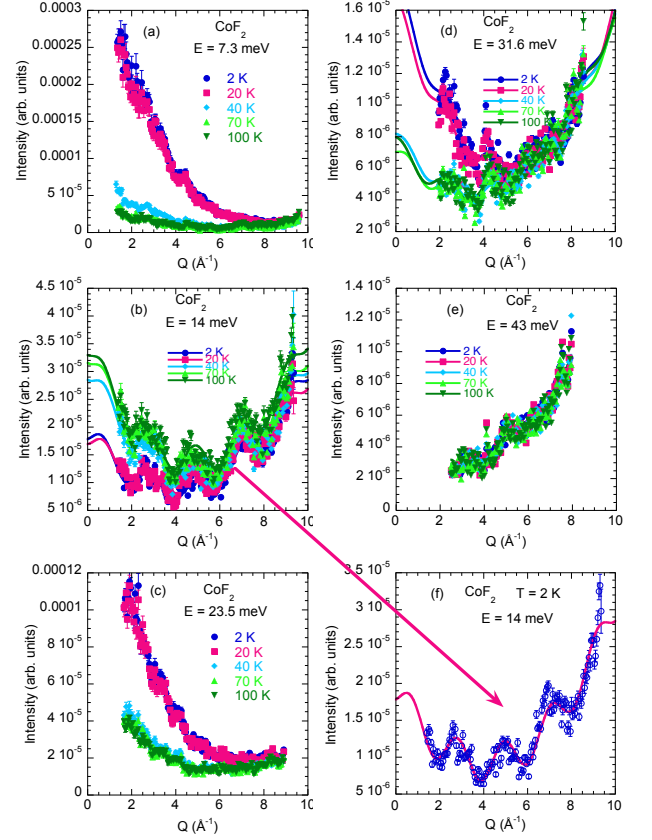


FIG. 7: Q dependence of the intensity for the inelastic peaks at $E = 7.3, 14.0, 23.5, 31.6$ and 43.0 meV at $T = 2, 20, 40, 70$ and 100 K ($\lambda_i = 1.1 \text{ \AA}$).

Both magnetic and structural excitations have been investigated^{27,28} by inelastic neutron scattering on CoF₂ single crystals. The magnetic properties of CoF₂ are much more complex than those of MnF₂ having the same rutile crystal structure and also the same antiferromagnetic structure. Crystal field calculations of Gladney³⁵ shows that the $L = 3, S = 3/2$ atomic ground state is split by the octahedral crystal field to give an orbital Γ_4 triplet as the ground state whose properties can be described by an effective $l = 1$ operator. The rhombic and tetragonal crystal field distortions and the spin-orbit coupling causes this state to split into six Kramers doublets. The molecular field in the antiferromagnetic phase causes further splitting. Labeling the ground state as A and first three excited states as B, C and D three crystal-field excitations have been labeled²⁷ as A-B, A-C and A-D transitions. Alternatively these states are also labeled²⁸ as 0, 1, 2, 3. The corresponding excitations are labeled as 0 - 1, 0 - 2 and 0 - 3. The dispersions of these excitations have been measured from single crystal samples along [100] and [001] directions. However, the anisotropy

in dispersion of these excitations is found to be rather small. The strongest excitation is A-B which is at about 7.4 meV for $q = 0$. The other two excitations are A-C and A-D that both lie at about 24-25 meV.

Fig. 2 shows the temperature evolution of the scattering function $S(Q, \omega)$ measured with incident neutron wavelength of $\lambda = 1.5 \text{ \AA}$ and Fig. 3 shows temperature evolution of the scattering function $S(Q, \omega)$ measured with $\lambda = 1.1 \text{ \AA}$. At $T = 2 \text{ K}$ we observe two inelastic peaks at about $E = 8 \text{ meV}$ and $E = 24 \text{ meV}$. The energy of these peaks decreases with increasing temperature. However whereas the energy of the first peak at $E = 8 \text{ meV}$ becomes almost zero at $T_N = 38 \text{ K}$, the energy of the second peak decreases and then attains a finite value at T_N and stays constant at about 19 meV at higher temperatures. Fig. 4 shows the results of the fit of the low-Q data from CoF₂ in the low-energy range in the left two panels. Two Gaussian peaks have been fitted to account for the elastic peak at zero energy and the inelastic peak which is at about $E = 8 \text{ meV}$ at $T = 2 \text{ K}$. The energy of the inelastic peak decreases with increasing temperature and becomes zero at $T_N = 38 \text{ K}$ giving rise to quasielastic scattering, which has been fitted with a Lorentzian function. The results of the fit with Gaussian functions to the higher-energy peaks are shown in Fig. 5. At low temperatures below $T_N = 38 \text{ K}$, three peaks could be identified and they were fitted with three Gaussian functions. At higher temperatures only a broad peak could be identified and has been fitted with a single Gaussian function. Fig. 6 (a) shows the temperature variation of the energy and the half-width at half-maximum (HWHM) of the low-energy inelastic magnetic peak of CoF₂. In Fig. 6 (b) the temperature variation of the energy of the higher-energy inelastic magnetic peak of CoF₂ has been shown. The temperature variation of the low energy inelastic peak which is at about 8 meV at 2 K shows clearly that this peak is due to magnetic excitations. The energy of this peak decreases continuously and becomes almost zero at $T_N = 38 \text{ K}$ giving rise to quasielastic scattering of Lorentzian form. The higher energy peak at about 24 meV on the other hand seems to be a hybrid peak due to the magnon-phonon coupling. The peak persists at temperature higher than T_N and its energy remains constant at about 19 meV.

Fig. 7 shows the Q dependence of the intensity for the inelastic peaks at $E = 7.3, 14.0, 23.5, 31.6$ and 43.0 meV at $T = 2, 20, 40, 70$ and 100 K . Fig. 7 (a) shows the Q dependence of the peak at $E = 7.3 \text{ meV}$ for several temperatures. The intensity of the peak at $E = 7.3 \text{ meV}$ at $T = 2 \text{ K}$ decreases continuously with increasing Q and then becomes more or less constant at higher Q. This indicates that the inelastic peak is of mostly magnetic origin. This is also supported by its intensity and Q dependence at $T = 100 \text{ K}$. However even at $T = 100 \text{ K}$ the intensity is not zero. This suggests that there exists some phonon contribution to this peak as well. The Q dependence at $T = 100 \text{ K}$ shows that the intensity increases slightly at higher Q and this also confirms that

there exist some phonon contribution to this peak. Fig. 7 (b) shows the Q dependence of the inelastic peak at $E = 14 \text{ meV}$ at several temperatures. The intensity of this peak first decreases with increasing Q and then increases very much at higher Q. This suggests that the peak has a hybrid phonon and magnon character. The Q dependence of such a hybrid peak is also expected to be more exotic. Fig. 7 (c) shows the Q dependence of the inelastic peak at $E = 23.5 \text{ meV}$. Its Q dependence is very similar to the peak at $E = 7.3 \text{ meV}$ shown in Fig. 7 (a). Even its temperature dependence is very similar. The intensity of the peak at all Q is higher at lower temperature. The decrease of its intensity with increasing Q suggests that it is magnon like. However like the peak at $E = 7.3 \text{ meV}$ the peak at $E = 23.5$ also shows slight tendency of increasing in intensity at higher Q suggesting that the peak has some phonon like character. Fig. 7 (d) shows the Q dependence of the inelastic peak at $E = 31.6 \text{ meV}$. It looks very similar to that at $E = 14 \text{ meV}$ and consists clearly of both phonon and magnon contributions. Lastly the Q dependence of the inelastic peak shown in Fig. 7 (e) shows that this peak is almost pure phonon like because its intensity increases with Q and temperature. We have fitted the Q dependence of the intensity for the peaks at 14 and 31.6 meV assuming them to consist of both magnon and phonon contributions and also assuming that the Q dependence has oscillatory cosine wave form due to the periodicity of the lattice. We fitted the intensity by the equation

$$I(Q) = a_1 + a_2Q + a_3Q^2 + a_4 \cos\left(\frac{2\pi}{a_5}Q + a_6\right) \quad (3)$$

which consists of a polynomial plus an oscillatory cosine function. Here $a_1, a_2,$ and a_3 are coefficients of a second order polynomial and a_4 is the amplitude and a_5 is the periodicity of the oscillatory part superimposed on the polynomial function and a_6 is the phase. This is a much simplified function but since it contains term proportional to Q describing Q dependence of the magnetic intensity and a term proportional to Q^2 describing the Q dependence of the phonon intensity and has also a superimposed oscillatory term describing the effect of lattice periodicity, it describes the intensity variation rather well. The fitted periodicity is in agreement with the average lattice periodicity. Since the fits for different temperature in Fig. 7 (b) is not clearly visible we show a typical fit at $T = 2 \text{ K}$ separately in Fig. 7 (f). The fit looks rather convincing indeed. In fact the Q dependences of the intensities for all five energies shown in Fig. 7 (a-f) show oscillations but the statistics and also the resolution of the data shown in Fig. 7 (a), 7 (c) and 7 (e) are not good enough for reasonable fits.

In conclusion we investigated the phonon and spin dynamics of CoF₂ by inelastic neutron scattering on powder samples by time-of-flight neutron spectroscopy with unpolarized neutrons. The temperature and the Q dependence of the intensity of the inelastic signals enabled us to identify their phonon, magnon or hybrid origin at least to

a first approximation. We note that there exist considerable phonon-magnon interaction in this simple antiferromagnetic system also evidenced by the strong magnetoelastic coupling observed by neutron diffraction³. How-

ever, in order to be certain about the hybrid nature of these inelastic peaks and evaluate quantitatively phonon-magnon interaction strength, polarized neutron scattering investigation is desirable.

-
- ¹ Spin waves, A.I. Akhiezer et. al., North-Holland, Amsterdam (1968) p. 134.
- ² M. Zbiri et al., J. Phys.: Condens. Matter **22**, 315701 (2010) and the references therein.
- ³ T. Chatterji, B. Ouladdiaf, T. Hansen, J. Phys.: Condens. Matter **22**, 096001 (2010).
- ⁴ T. Chatterji, G.N. Iles, B. Ouladdiaf, T. Hansen, J. Phys.: Condens. Matter **22**, 316001 (2010).
- ⁵ R.M. Macfarlane and H. Morawitz, Phys. Rev. Lett. **27**, 151 (1971).
- ⁶ M.T. Hutchings et al., Phys. Rev. B **2**, 1362 (1970)
- ⁷ I.D. Mayergoyz, *Handbook of Giant Magnetoresistive Materials*, Academic Press, San Diego (2000).
- ⁸ E. du Tremolet de Lacheisserie, *Magnetostriction: Theory and Application of Magnetoelasticity*, CRC Press, Boca Raton (1993).
- ⁹ P. Morin and D. Schmitt, in *Ferromagnetic Materials*, Vol. 5, ed. K.H.J. Buschow and E.P. Wohlfarth, Elsevier, Amsterdam (1990), p. 59.
- ¹⁰ S. Andreev, in *Ferromagnetic Materials*, Vol. 5, ed. K.H.J. Buschow and E.P. Wohlfarth, Elsevier, Amsterdam (1990), p. 237.
- ¹¹ E.F. Wassermann, in *Ferromagnetic Materials*, Vol. 5, ed. K.H.J. Buschow and E.P. Wohlfarth, Elsevier, Amsterdam (1990), p. 1.
- ¹² A.E. Clark in *Ferromagnetic Materials*, Vol. 1, ed. E.P. Wohlfarth, North-Holland Publishing Company, Amsterdam (1980), p. 531
- ¹³ B. Morosin, Phys. Rev. B **1**, 236 (1970).
- ¹⁴ M. Doerr, M. Rotter and A. Lindbaum, Adv. Phys. **54**, 1 (20050).
- ¹⁵ A. Lindbaum and M. Rotter, in *Handbook of Magnetic Materials*, Vol. 14, ed. K.H.J. Buschow, Elsevier, Amsterdam (2002), p. 307
- ¹⁶ T. Chatterji, P.F. Henry and B. Ouladdiaf, Phys. Rev. B **77**, 212403 (2008).
- ¹⁷ T. Chatterji, B. Ouladdiaf and D. Bhattacharya, J. Phys: Condens. Matter **21**, 306001 (2009).
- ¹⁸ J.W. Staut and M. Griffel, Phys. Rev. **76**, 144 (1949).
- ¹⁹ R.C. Ohlmann and M. Tinkham, Phys. Rev. **123**, 425 (1961).
- ²⁰ F. Kieffer, Phys. Rev. **87**, 608 (1952).
- ²¹ T. Nakamura, and H. Taketa, Progr. Theoret. Phys., (Kyoto) **13**, 129 (1955).
- ²² J.W. Staut, and L.M. Matarrese, Rev. Mod. Phys., **25**, 338 (1953).
- ²³ T. Moriya, J. Phys. Chem. Solids, **11**, 73 (1959).
- ²⁴ V. Jaccarino, Phys. Rev. Lett. **2**, 163 (1959).
- ²⁵ V. Jaccarino, J. Chem. Phys. **30**, 1627 (1959).
- ²⁶ R.A. Erickson, Phys. Rev. **90**, 779 (1953).
- ²⁷ P. Martel, R.A. Cowley, and R.W.H. Stevenson, Can. J. Phys. **46**, 1355 (1968).
- ²⁸ R.A. Cowley, W.J.L. Buyers, P. Martel, and R.W.H. Stevenson, J. Phys. C: Solid State Phys. **6**, 2997 (1973).
- ²⁹ J. Stempfer, U. Rütt, S. P. Bayracki, T. Brückel and W. Jauch, Phys. Rev. B **69**, 014417 (2004).
- ³⁰ W. Jauch, M. Reehuis, and A.J. Schultz, Acta Cryst. **A60**, 51 (2004).
- ³¹ *Neutron Scattering from Magnetic Materials*, ed. T. Chatterji, Elsevier, Amsterdam (2006).
- ³² T. Chatterji and G.J. Schneider, J. Phys.: Condens. Matter **21**, 436008 (2009).
- ³³ G.L. Squires, *Introduction to the theory of thermal neutron scattering*, Cambridge University Press, Cambridge (1978).
- ³⁴ W. Marshall and S.W. Lovesey, *Theory of thermal neutron scattering*, Clarendon Press, Oxford (1971).
- ³⁵ H.M. Gladney, Phys. Rev. **146**, 253 (1966)